

Evolution in the iron abundance of the ICM

Italo BALESTRA¹, Paolo TOZZI, Stefano ETTORI, Piero ROSATI, Stefano BORGANI,
Vincenzo MAINIERI and Colin NORMAN

¹*Max-Planck-Institut für Extraterrestrische Physik, Postfach 1312, 85741
Garching, Germany*

We present a Chandra analysis of the X-ray spectra of 56 clusters of galaxies at $z > 0.3$, which cover a temperature range of $3 > kT > 15$ keV. Our analysis is aimed at measuring the iron abundance in the ICM out to the highest redshift probed to date. We find that the emission-weighted iron abundance measured within $(0.15 - 0.3) R_{vir}$ in clusters below 5 keV is, on average, a factor of ~ 2 higher than in hotter clusters, following $Z(T) \simeq 0.88 T^{-0.47} Z_{\odot}$, which confirms the trend seen in local samples. We made use of combined spectral analysis performed over five redshift bins at $0.3 > z > 1.3$ to estimate the average emission weighted iron abundance. We find a constant average iron abundance $Z_{Fe} \simeq 0.25 Z_{\odot}$ as a function of redshift, but only for clusters at $z > 0.5$. The emission-weighted iron abundance is significantly higher ($Z_{Fe} \simeq 0.4 Z_{\odot}$) in the redshift range $z \simeq 0.3 - 0.5$, approaching the value measured locally in the inner $0.15 R_{vir}$ radii for a mix of cool-core and non cool-core clusters in the redshift range $0.1 < z < 0.3$. The decrease in Z_{Fe} with z can be parametrized by a power law of the form $\sim (1 + z)^{-1.25}$. The observed evolution implies that the average iron content of the ICM at the present epoch is a factor of ~ 2 larger than at $z \simeq 1.2$. We confirm that the ICM is already significantly enriched ($Z_{Fe} \simeq 0.25 Z_{\odot}$) at a look-back time of 9 Gyr. Our data provide significant constraints on the time scales and physical processes that drive the chemical enrichment of the ICM.

§1. Properties of the sample and spectral analysis

The selected sample consists of all the public *Chandra* archived observations of clusters with $z \geq 0.4$ as of June 2004, including 9 clusters with $0.3 < z < 0.4$. We used the XMM-*Newton* data to boost the S/N only for the most distant clusters in our current sample, namely the clusters at $z > 1$.

The spectrum of each cluster is extracted from a circular region whose radius maximizes the S/N. As shown in Fig. 1, in most cases the extraction radius R_{ext} is between 0.15 and $0.3 R_{vir}$. The spectra were fitted with a single-temperature model in which the ratio between the elements was fixed to the solar value.¹⁾

We show in Fig. 1 the distribution of temperatures in our sample as a function of redshifts (error bars are at the 1σ c.l.). The Spearman test shows no correlation between temperature and redshift ($r_s = -0.095$ for 54 d.o.f., probability of null correlation $p = 0.48$). Fig. 1 shows that the range of temperatures in each redshift bin is about 6–7 keV. Therefore, we are sampling a population of medium-hot clusters uniformly with z , with the hottest clusters preferentially in the range $0.4 < z < 0.6$.

Our analysis suggests higher iron abundances at lower temperatures in all the redshift bins. This trend is somewhat blurred by the large scatter. We find a more than 2σ negative correlation for the whole sample, with $r_s = -0.31$ for 54 d.o.f. ($p = 0.018$). The correlation is more evident when we compute the weighted average of Z_{Fe} in 6 temperature intervals, as shown by the shaded areas in Fig. 2.

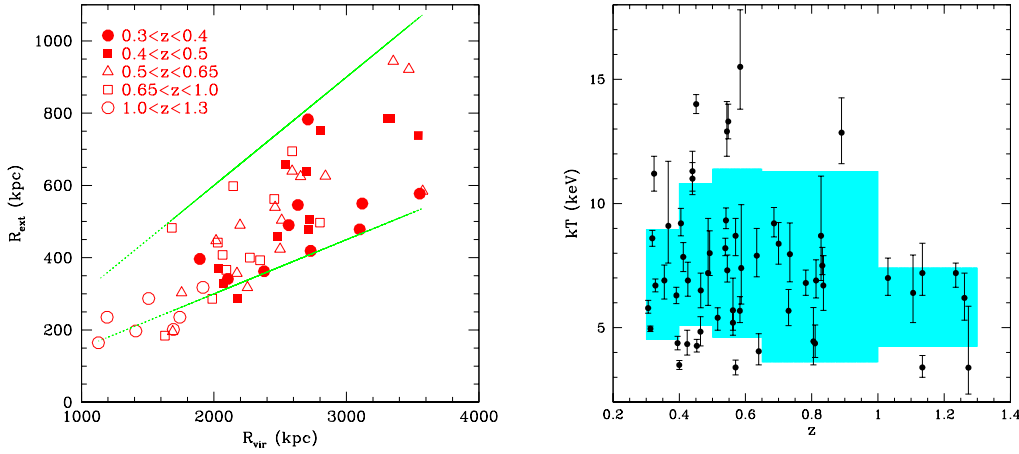


Fig. 1. *Left*: extraction radius R_{ext} versus R_{vir} . Lower and upper lines show $R_{ext} = 0.15 R_{vir}$ and $R_{ext} = 0.3 R_{vir}$, respectively. *Right*: temperature vs redshift. Shaded areas show the rms dispersion around the weighted mean in different redshift bins.

§2. The evolution of the iron abundance with redshift

The single-cluster best-fit values of Z_{Fe} decrease with redshift. We find a $\sim 3\sigma$ negative correlation between Z_{Fe} and z , with $r_s = -0.40$ for 54 d.o.f. ($p = 0.0023$). The decrease in Z_{Fe} with z becomes more evident by computing the average iron abundance as determined by a *combined spectral fit* in a given redshift bin. We performed a simultaneous spectral fit leaving temperatures and normalizations free to vary, but using a single metallicity for the clusters in a narrow z range.

The Z_{Fe} measured from the *combined fits* in 6 redshift bins is shown in Fig. 2. We also computed the weighted average from the single cluster fits in the same redshift bins. The best-fit values resulting from the *combined fits* are always consistent with the weighted means within 1σ (see Fig. 2). This allows us to measure the evolution of the average Z_{Fe} as a function of redshift, which can be modelled with a power law of the form $\sim (1 + z)^{-1.25}$.

Since the extrapolation of the average Z_{Fe} at low- z points towards $Z_{Fe}(0) \simeq 0.5 Z_{\odot}$, we need to explain the apparent discrepancy with the oft-quoted canonical value $\langle Z_{Fe} \rangle \simeq 0.3 Z_{\odot}$. The discrepancy is due to the fact that our average values are computed within $r \simeq 0.15 R_{vir}$, where the iron abundance is boosted by the presence of metallicity peaks often associated to cool cores. The regions chosen for our spectral analysis, are larger than the typical size of the cool cores, but smaller than the typical regions adopted in studies of local samples. In order to take into account aperture effects, we selected a small subsample of 9 clusters at redshift $0.1 < z < 0.3$, including 7 cool-core and 2 non cool-core clusters, a mix that is representative of the low- z population. Here we analyze the X-ray emission within $r = 0.15 R_{vir}$ in order to probe the same regions probed at high redshift. We used

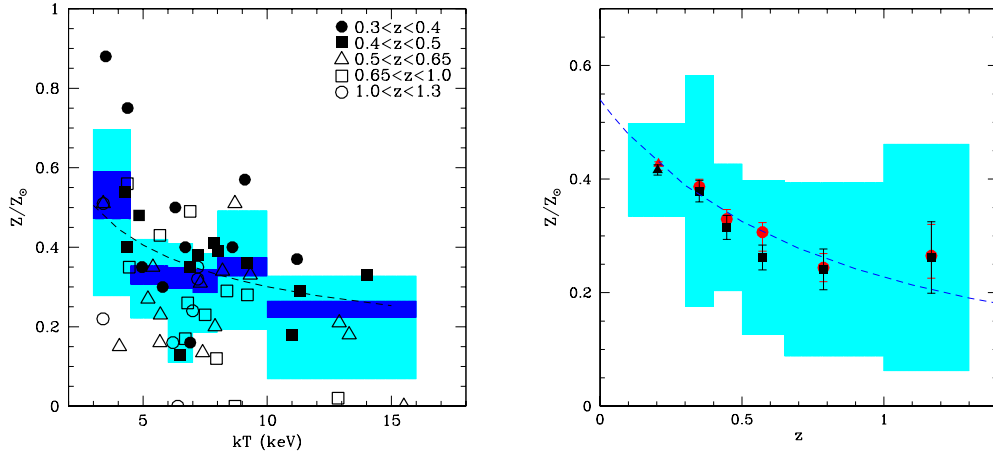


Fig. 2. *Left:* scatter plot of best-fit Z_{Fe} values versus kT . The dashed line represents the best-fit $Z-T$ relation ($Z/Z_{\odot} \simeq 0.88 T^{-0.47}$). Shaded areas show the weighted mean (blue) and average Z_{Fe} with rms dispersion (cyan) in 6 temperature bins. *Right:* mean Z_{Fe} from combined fits (red circles) and weighted average of single-source measurements (black squares) within 6 redshift bins. The triangles at $z \simeq 0.2$ are based on the low- z sample described in Sect. 2. Error bars refer to the 1σ c.l.. Shaded areas show the rms dispersion. The dashed line indicates the best fit over the 6 redshift bins for a simple power law of the form $\langle Z_{Fe} \rangle = Z_{Fe}(0) (1+z)^{-1.25}$.

this small control sample to add a low- z point in our Fig. 2, which extends the Z_{Fe} evolutionary trend.

§3. Conclusions

We have presented the spectral analysis of 56 clusters of galaxies at intermediate-to-high redshifts observed by *Chandra* and *XMM-Newton*.²⁾ This work improves our first analysis aimed at tracing the evolution of the iron content of the ICM out to $z > 1$,⁴⁾ by substantially extending the sample. The main results of our work can be summarized as follows:

- We determine the average ICM iron abundance with a $\sim 20\%$ uncertainty at $z > 1$ ($Z_{Fe} = 0.27 \pm 0.05 Z_{\odot}$), thus confirming the presence of a significant amount of iron in high- z clusters. Z_{Fe} is constant above $z \simeq 0.5$, the largest variations being measured at lower redshifts.
- We find a significantly higher average iron abundance in clusters with $kT < 5$ keV, in agreement with trends measured in local samples. For $kT > 3$ keV, Z_{Fe} scales with temperature as $Z_{Fe}(T) \simeq 0.88 T^{-0.47}$.
- We find significant evidence of a decrease in Z_{Fe} as a function of redshift, which can be parametrized by a power law $\langle Z_{Fe} \rangle \simeq Z_{Fe}(0) (1+z)^{-\alpha_z}$, with $Z_{Fe}(0) \simeq 0.54 \pm 0.04$ and $\alpha_z \simeq 1.25 \pm 0.15$. This implies an evolution of more than a factor of 2 from $z = 0.4$ to $z = 1.3$.

We carefully checked that the extrapolation towards $z \simeq 0.2$ of the measured trend, pointing to $Z_{Fe} \simeq 0.5 Z_{\odot}$, is consistent with the values measured within a radius $r = 0.15 R_{vir}$ in local samples including a mix of cool-core and non cool-core clusters. We also investigated whether the observed evolution is driven by a negative evolution in the occurrence of cool-core clusters with strong metallicity gradients towards the center, but we do not find any clear evidence of this effect. We note, however, that a proper investigation of the thermal and chemical properties of the central regions of high- z clusters is necessary to confirm whether the observed evolution by a factor of ~ 2 between $z = 0.4$ and $z = 1.3$ is due entirely to physical processes associated with the production and release of iron into the ICM, or partially associated with a redistribution of metals connected to the evolution of cool cores.

Precise measurements of the metal content of clusters over large look-back times provide a useful fossil record for the past star formation history of cluster baryons. A significant iron abundance in the ICM up to $z \simeq 1.2$ is consistent with a peak in star formation for proto-cluster regions occurring at redshift $z \simeq 4 - 5$. On the other hand, a positive evolution of Z_{Fe} with cosmic time in the last 5 Gyrs is expected on the basis of the observed cosmic star formation rate for a set of chemical enrichment models. Present constraints on the rates of SNaI type Ia and core-collapse provide a total metal production in a typical X-ray galaxy cluster that well reproduce (i) the overall iron mass, (ii) the observed local abundance ratios, and (iii) the measured negative evolution in Z_{Fe} up to $z \simeq 1.2$.³⁾

References

- 1) Anders, E. & Grevesse, N. 1989, *Geochim. Cosmochim. Acta*, 53, 197
- 2) Balestra, I., Tozzi, P., Ettori, S., et al. 2007, *A&A*, 462, 429
- 3) Ettori, S. 2005, *MNRAS*, 362, 110
- 4) Tozzi, P., Rosati, P., Ettori, S., et al. 2003, *ApJ*, 593, 705